ELSEVIER

Marine Chemistry 52 (1996) 55–73

MARINE CHEMISTRY

Phosphorus binding by poorly crystalline iron oxides in North Sea sediments

C.P. Slomp *, S.J. Van der Gaast, W. Van Raaphorst

Netherlands Institute for Sea Research (NIOZ), P.O. Box 59, 1790 AB Den Burg (Texel), The Netherlands

Received 3 April 1995; accepted 1 November 1995

Abstract

Differential X-ray powder diffraction (DXRD) and extraction procedures were used to characterize the iron oxides present in four sediments from contrasting environments in the North Sea. Stations were located in depositional areas on the southern shelf (German Bight) and on the north-eastern shelf-slope transition (Skagerrak) and in areas with no net deposition in the southern North Sea. Poorly crystalline ferrihydrite and akageneite (extractable with 0.1 M HCl and 0.2 M NH_4-oxalate) were identified in the fine sediment fraction (< 10 μm) of surface samples at all locations. Evidence for the dominant role of these Fe oxides in the binding of phosphorus in North Sea sediments was obtained from the good relationship of both the content of Fe-bound P and the linear adsorption coefficient for phosphate with NH_4-oxalate extractable Fe. A tight coupling of pore water Fe^{2+} and HPO_4^{2-} was observed at 3 stations. Pore water Fe^{2+}/HPO_4^{2-} ratios at maximum pore water concentrations of Fe^{2+} were similar to NH_4-oxalate Fe/Fe-bound P ratios for surface sediment at these locations, and were in the range known for synthetic poorly crystalline Fe oxides. This suggests that pore water HPO_4^{2-} production at the time of core collection was dominated by release from poorly crystalline Fe oxides. In contrast, at the German Bight station, much higher HPO_4^{2-} levels and a decoupling of pore water Fe^{2+} and HPO_4^{2-} was observed, suggesting a larger contribution of mineralization of organic matter to pore water HPO_4^{2-} than at the other sites. Solid phase P analyses indicate possible redistribution of Fe-bound P to another inorganic phase at depth at the Skagerrak station, but not at the other stations. The persistence with depth of poorly crystalline Fe oxides and Fe-bound P suggests that these Fe phases can act as both a temporary and permanent sink for P in continental margin sediments.

1. Introduction

Iron oxides, hydroxides and oxyhydroxides (henceforth called Fe oxides) can provide sorption sites for compounds with a high affinity for the Fe oxide surface such as many trace metals, silica and phosphorus (P). The large effect of these sorption processes on the cycling of P in marine sediments is well-documented. Fe oxides present in the oxidized surface layer of the sediment can act as a "trap" for pore water HPO_4^{2-} diffusing upwards (Krom and Berner, 1980; Sundby et al., 1992; Slomp and Van Raaphorst, 1993). Rapid sorption and release of P from "reactive" Fe oxides can control pore water HPO_4^{2-} concentrations and thus directly affect sediment–water exchange (Sundby et al., 1992; Van Raaphorst and Kloosterhuis, 1994). Simultaneous release of P and fluoride from Fe oxides may provide the necessary conditions for early diagenetic carbonate fluorapatite (CFA) precipitation (Ruttenberg and

* Corresponding author.

SSDI 0304-4203(95)00078-X

Berner, 1993). The persistence of some Fe oxides with depth, as has been observed in many marine sediments (e.g. Sundby et al., 1992; Jensen and Thamdrup, 1993; Kostka and Luther, 1994), enables Fe-bound P to become an important permanent reservoir for P in marine sediments (Ruttenberg, 1993). As the mineralogy and crystallinity of Fe oxides strongly influence their HPO_4^{2-} sorption characteristics (Borggaard, 1983a; Parfitt, 1989; Ruttenberg, 1992) and their susceptibility to reduction (Schwertmann, 1991), knowledge of the character of these Fe phases in marine sediments is essential for a correct understanding of their role in the P cycle.

The reported occurrences of Fe oxides in the marine environment compiled by Murray (1978) and Burns and Burns (1980) mostly apply to concretions or nodules found in deep sea sediments. Very little is known about the mineral forms of Fe oxides in coastal marine sediments. Direct determination with conventional techniques (e.g. X-ray powder diffraction, X-ray microanalysis) is difficult which is due to their low concentrations, their (presumably) poor crystallinity, and the fact that they are generally present as coatings on other particles. As an alternative, extraction techniques which have been tested for their selectivity using pure mineral phases are widely employed (e.g. Canfield, 1988; Canfield, 1989; Kostka and Luther, 1994). When applied to natural materials these techniques are only operationally defined. Firstly, extractants always suffer from a lack of absolute specificity in mineral or phase separation. Secondly, mineral phases in sediments may have very different solubilities compared to the standard materials used for calibration, e.g., due to another mode and environment of formation and variations in the extent of weathering prior to deposition.

Sequential X-ray powder diffraction measurements in combination with extraction schemes (differential XRD: DXRD) partly circumvent the above mentioned problems by lowering the detection limit for Fe oxides and making direct identification of extracted phases possible (Schulze, 1981; Van der Gaast, 1991; Wang et al., 1993). In this study the DXRD technique is applied to the fine sediment fraction (< 10 μm) of surface samples from four contrasting environments in the North Sea with the aim of identifying the Fe oxides present. The DXRD results are combined with bulk sediment solid phase speciation (determined using extraction procedures) and pore water profiles of Fe^{2+} and HPO_4^{2-} to determine whether the identified Fe oxides are responsible for the binding of P in these sediments. The results show that poorly crystalline akageneite and ferrihydrite are the most important Fe oxides in these continental margin sediments and that these Fe phases are responsible for the binding of P.

2. Materials and methods

2.1. Study sites and sample collection

The North Sea is a semi-enclosed part of the north–west European shelf with water depths gradually increasing from less than 30 m in the south to about 200 m in the area between the Shetlands and the Norwegian coast. To the northeast, in the Skagerrak/Norwegian channel, the seafloor slopes down to a depth of 700 m. The water circulation and transport of suspended matter are predominantly counterclockwise (Fig. 1). Net sedimentation of material is negligible outside the deposition areas of the inner German Bight and the Skagerrak/Norwegian Channel (Eisma and Kalf, 1987), where estimated sedimentation rates vary between 0.5 and 1 cm yr^{-1} (Von Haugwitz et al., 1988; Eisma and Kalf, 1987) and between 0.1 and 0.5 cm yr^{-1} (Van Weering et al., 1987; Anton et al., 1993), respectively. An estimated 50 to 70% of total North Sea suspended matter eventually is deposited in the Skagerrak/Norwegian Channel (Eisma and Kalf, 1987). Local sources of suspended matter, due to past dredging and dumping of harbour sludge, may be of some importance in the German Bight (Irion et al., 1987). In contrast to the Skagerrak area, large seasonal variations in deposition and mineralization rates of organic matter occur in the German Bight area, leading to sediment anoxia in summer (Lohse et al., 1995).

Four locations with a wide range of sediment characteristics (Table 1) were selected for this study. Stations 9 and 13 (medium silt) are located in the main depositional areas (Skagerrak and German Bight), whereas stations 5 and 14 (fine sand) are both located in areas with no net deposition. Station 14 lies right outside the German Bight depositional area.

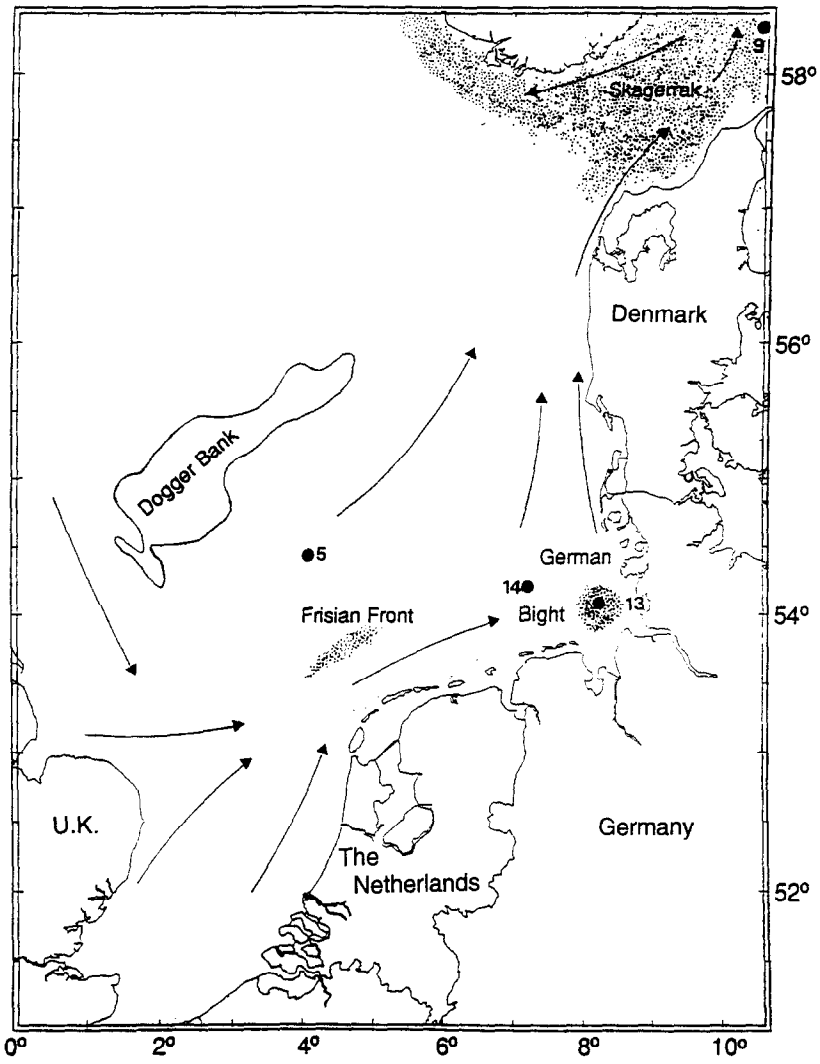

Fig. 1. Map of the North Sea showing the sampling locations and station numbers. Main transport routes of water and suspended matter in the North Sea are indicated (arrows). Stippled areas indicate main depositional regions.

Table 1
Location, depth and some general characteristics of the sediment at the sampling locations (median grain size determined in the upper 0–0.5 cm of the sediment, all other parameters are averages for the 0–1.0 cm layer). Sediment classification is based on the Wentworth size scale (Pettijohn and Potter, 1972)

St. nr.	Location		Water depth (m)	Porosity (v/v)	Org. C (%)	Org. N (%)	Org.P (%)	$CaCO_3$ (%)	$< 10\ \mu m$ fraction (%)	Median grain size (μm)	Sediment classification
	Lat. N	Long. E									
5	54.25	4.04	49	0.49	0.17	0.027	0.0023	1.7	8	103	very fine sand
9	58.20	10.27	330	0.89	2.83	0.338	0.0291	9.6	72	6	medium silt
13	54.05	8.09	19	0.64	0.82	0.097	0.0108	10.3	42	15	medium silt
14	54.14	7.20	39	0.56	0.36	0.047	0.0050	6.5	7	98	very fine sand

In February 1992 sediment cores were obtained with a cylindrical box corer (31 cm i.d.) which enclosed 30 to 50 cm of sediment column together with 15 to 25 l of overlying bottom water. Subsamples were taken from the box core with acrylic liners which were closed with rubber stoppers. Only cores without any visible surface disturbance were used. At all stations a brown surface layer was observed, varying in thickness from ~ 5–7 cm (st. 5, 13, 14) to ~ 10 cm (st. 9). The underlying sediment was either black (st. 13), brown/black (st. 5, 9) or grey/black (st. 14).

2.2. *Pore water and solid phase analysis*

To obtain pore water, sediment from 10–15 subcores (i.d. 3.1 cm) was sliced in a nitrogen flushed box immediately after collection. Slices from 9 depth intervals (0–0.4, 0.4–1, 1–1.5, 1.5–2, 2–3, 3–4, 4–6, 6–8, 8–10 cm) were pooled in teflon centrifuge tubes with a built-in filter specially designed for sandy, low porosity sediments (Saager et al., 1990) at stations 5 and 14, and in 50 ml polypropylene centrifuge tubes at stations 9 and 13. These were centrifuged for 10 min at 1700 *g*. The filtered (cellulose acetate, 0.45 μm) samples were acidified to pH ≈ 1 and stored at 4°C until analysis for HPO_4^{2-}, Fe^{2+} and Mn^{2+}. All sample manipulations took place at in situ temperature (4.4 to 6.4°C).

Sliced sediment from 8–10 additional subcores was pooled and stored frozen (−20°C) until solid phase analysis. Sediment from 7 depth intervals (0–0.5, 0.5–1, 1–2, 2–4, 4–6, 6–8, 8–12 cm) was subjected to five (non-sequential) extraction procedures for Fe: (1) 0.1 M HCl for 18 h (Duinker et al., 1974); (2) 1 M HCl for 24 h (Canfield, 1988); (3) 0.2 M NH_4-oxalate/oxalic acid buffer (pH 3.0) for 2 h under oxic conditions in the dark (Schwertmann and Cornell, 1991); (4) 0.5 M oxalic acid for 2 h (pH 1.7) (Schwertmann and Cornell, 1991); (5) citrate–

Table 2
Percentages of Fe extracted from common Fe-containing phases as determined either directly or estimated using standard minerals and four types of extraction solutions under various extraction conditions

Mineral	Oxalate		1 M HCl		Oxalic ac.		Dithionite	
	% Fe	Ref.	% Fe	Ref.	% Fe	Ref.	% Fe	Ref.
Amorphous Fe oxide	40–70	b	34–72	b	95	b		
Ferrihydrite ($Fe_5HO_8 \cdot 4H_2O$)	47–82, 70–80, 100	d,f,ag	100	a			100	a,l,g
Akageneite (β-FeOOH)	< 3, +	f,e						
Lepidocrocite (γ-FeOOH)	< 2, 42, 50	f,d,a	7	a			100	a
Goethite (α-FeOOH)	< 1, < 3, 35	gab,f,b	< 0.5, < 3	b,a	4–6	b	60–93, 100	fikg,a,l
Hematite (α-Fe_2O_3)	< 1, < 5	gab,f	< 0.5, < 3	b,a	7–12	b	5–30, 63, 98, 100	f,g,a,kl
Magnetite (Fe_3O_4)	20, 60, 70, 95	b,g,f,a	< 0.5, < 3	b,a	28–35,100	b,m	3, 90	a,g
Amorphous FeS	100	g	100	c			100	g
Mackinawite (FeS)			92	c				
Siderite ($FeCO_3$)								
Greigite (Fe_3S_4)			40–67	c				
Pyrite (FeS_2)			0	c			–	h
Chlorite	< 3, 3	a,g	32	a			2, 5, 7	i,g,a
Smectite	–	j					–	j
Vermiculite							+	k
Nontronite	< 3	a	7	a			27	a
Illite	–	j					–	j
Glauconite	< 3	a	10	a			10	a
Biotite	< 3	a	22	a				
Garnet	< 3	a	< 3	a			< 3	a

Key to the references: (a) Canfield, 1988; (b) Chao and Zhuo, 1983; (c) Cornwell and Morse, 1987; (d) Karim, 1984; (e) Kauffman and Hazel, 1975; (f) Kodama and Ross, 1991 (g) Kostka and Luther, 1994; (h) Lord, 1982; (i) Lucotte and d'Anglejan, 1985; (j) McKeague and Day, 1966; (k) Mehra and Jackson, 1960; (l) Ruttenberg, 1992; (m) Schwertmann and Cornell, 1991. + and − indicate substantial and minor dissolution, respectively, but % Fe extracted unknown. Letters not subdivided by commas refer to the same percentage in the table.

dithionite–bicarbonate solution (CDB, pH 7.3, 8 h, 20°C) (Ruttenberg, 1992). We tested the effect of the use of a higher temperature (70°C) and a shorter extraction time (15 min) as suggested in the original procedure for CDB-extractable Fe (Mehra and Jackson, 1960) using surface sediment from stations 5 and 9. We found no significant difference with the 8 h extraction at room temperature (20°C), even upon repeated (2 ×) extraction. Oven-dried (60°C), ground (teflon mortar and pestle) material was used for the HCl extractions. Untreated, wet sediment was used for all other procedures. Oven-drying may lead to phase modification and transformation of particularly poorly crystalline Fe oxides, and this may result in changes in their solubility (Schwertmann and Cornell, 1991). We checked whether this occurred at our relatively low oven-temperature by extracting both oven-dried and wet surface sediment from station 5 with 1 M HCl. We found no significant difference between the quantities of Fe extracted. All extraction procedures were performed with sediment under oxic conditions, therefore all Fe profiles include oxidized FeS. We have no data on FeS in these sediments, but based on results of other studies on Fe in North Sea sediments (Jørgensen, 1989; Canfield et al., 1993) we assume that FeS accounted for less than 10% of CDB-Fe.

Table 2 gives an overview of the percentages of Fe that are extracted from common Fe-containing phases as determined using standard minerals and four types of extraction solutions with similar active components (i.e. oxalic acid, 1 M HCl, oxalate and dithionite) to those applied in this study. A part of the observed variation in the efficiency of the extractions can be attributed to differences in the extraction conditions used in each study (extraction time, buffer system, etc.). Oxalate extractable Fe is often used as a rough indication of the amount of poorly crystalline Fe oxides in a sediment. 1 M HCl would be expected to additionally extract Fe from clay minerals. Although no evidence from experiments with standard minerals are available, oxalic acid may also extract clay mineral Fe (due to its low pH) and would be expected to give results comparable to 1 M HCl. Dithionite extractable Fe should give a measure for total Fe oxide Fe. No tests of 0.1 M HCl extractions with standard minerals are known, but it is assumed to extract the same phases as 1 M HCl with less attack on clay minerals (Duinker et al., 1974).

CDB-extractable P is used as a measure for total Fe-bound P (Ruttenberg, 1992). Inorganic and total P were determined as 1 M HCl-extractable P (24 h) before and after ignition of the sediment at 550°C (2 h). The difference between total and inorganic P is used as a measure for organic-P (Aspila et al., 1976; Ruttenberg, 1992). Dilute (0.1 M) HCl, NH_4-oxalate, and oxalic acid extractions can partially solubilize apatite P (Lucotte and d'Anglejan, 1985) and P attached to surfaces of crystalline Fe oxides. Therefore it is not possible to differentiate directly between P bound to different types of Fe oxides with these extractions.

Porosity was determined by weight loss of the sediment after drying at 60°C for 48 h and assuming a specific sediment weight of 2.65 kg dm^{-3}. Grain size distribution was determined with a Malvern particle analyzer. Total C and N and organic C were measured with a Carlo Erba 1500-2 elemental analyzer (Verardo et al., 1990). All sediment N was assumed to be in an organic form. $CaCO_3$ contents were calculated from inorganic C contents. A good correlation with $CaCO_3$ values calculated from 1 M HCl extractable Ca was found (HCl-$CaCO_3$ = 0.93 × Inorg.C-$CaCO_3$ + 0.11; R^2 = 0.93).

2.3. Differential X-ray powder diffraction

The < 10 μm fraction of surface sediment from all four stations was used for the XRD analysis for two reasons. Firstly, Fe oxides are expected to be mostly present in the fine sediment fraction, either in the form of coatings on other particles such as clay minerals or as very small crystals (5–150 nm in size; Schwertmann, 1991). Secondly, the particle size of substances analyzed with XRD is preferred to be below 10 μm (Van der Gaast, 1991).

In order to concentrate the Fe oxides the < 10 μm fraction of sediment from 0.5–1.0 cm depth (insufficient material was available from the 0–0.5 cm depth layer) was separated by repeated centrifugation and resuspension. Microscopic examination (1000 × magnification) showed that very few particles larger than 10 μm were present indeed. Calcium carbonate was removed by a 1 h extraction with 1 M sodium acetate buffer (pH 5) to prevent the forma-

tion of a Ca-oxalate complex during extraction with oxalic acid or NH_4-oxalate. The XRD characteristics of smectites depend on the type of cation that they hold in their exchange sites. To ensure that the exchange sites of the sediment smectites were always saturated with Ca, the sediment was exchanged with Ca using a $CaCl_2$ solution after each extraction step. This was followed by a rinse to remove the excess Ca. An ethanol–water mixture (1/1) was used for this rinse, to minimize hydrogen ion substitution for the exchangeable Ca (Moore and Reynolds, 1989). XRD analysis was performed on vacuum dried samples before and after each extraction. The sediment portions from each station were extracted non-sequentially with NH_4-oxalate and oxalic acid. The sample from station 5 was also extracted with 0.1 M HCl. Only following the oxalic acid extraction the sediment residues were subjected to two sequential CDB-extractions.

Randomly oriented specimens were prepared by gently pressing ~ 10 mg of sample material in a depression of a monocrystalline Si-disc which provides a very low background and no diffraction peaks. The XRD analysis was carried out using CoK α-radiation (40 kV, 40 mA) and a wide angle goniometer (PW 1050/25, Philips). The apparatus was equipped with a long fine focus X-ray tube, a graphite monochromator and a vacuum-helium device. Further details on instrumentation and methodology are given by Van der Gaast (1991).

DXRD patterns were obtained by subtraction of the XRD pattern after treatment from that before treatment. The patterns were normalized by calculating an intensity-ratio from a part of the pattern between 15 and 18° 2θ, from which only incoherent radiation was detected. After subtraction, the patterns were smoothed over nine points of equal weight. The removal of Fe oxides from sediments often results in an improved orientation of clay minerals (Moore and Reynolds, 1989). This causes an increase in their $00l$ (i.e. the diagnostic reflections used for the identification of the clay minerals) and a decrease in their *hk* (non-diagnostic) reflections. As a consequence, subtraction results in negative and positive peaks in the DXRD pattern, at the positions of the diagnostic and non-diagnostic reflections, respectively. These positive peaks are thus not indicative of clay mineral dissolution but solely reflect the change in clay mineral orientation. The same holds for positive peaks in the DXRD pattern for feldspar and quartz.

Due to a strong shift in the reflections of smectite as a result of NH_4 fixation in all samples extracted with NH_4-oxalate, interpretation of the matching XRD and DXRD diagrams was not possible (also see Kodama and Ross, 1991). We tried using Na-oxalate as an alternative, but found that a precipitate was formed when making a 0.2 M buffer solution of pH 3. Consequently, DXRD could only be applied to the 0.1 M HCl, oxalic acid and CDB extracted sediments.

2.4. Chemical analysis

Total Fe and Mn in the pore water (mostly present as Fe^{2+} and Mn^{2+}), Fe and Mn in the sediment extracts, and Ca in the 1 M HCl extracts were determined with a Perkin Elmer 5100 PC Atomic Absorption Spectrophotometer. Pore water HPO_4^{2-} and 1 M HCl-extractable P were determined on a Shimadzu Double beam Spectrophotometer with the method of Strickland and Parsons (1972). Total Fe, Al, Si and P in the NH_4-oxalate, the oxalic acid and the CDB solutions and in the DXRD–0.1 M HCl solution for station 5 were determined with an ICP Spectroflame (Spectro Analytical Instruments). Oxalic acid extractable elements were only analyzed for three sediment depths (5–10, 20–40, 60–80 mm). There was a good agreement between the Fe analysis with the AAS and ICP ($R^2 = 0.93$). Reproducibility of the analysis of the pore water and of the sediment extractions of bulk samples and of the < 10 μm fraction was generally better than 4%, 5% and 15%, respectively. The relatively large variation for the extractions of the fine material can be explained by the larger effect of sample heterogeneity when using small quantities of sample.

3. Results

3.1. Differential X-ray powder diffraction (< 10 μm fraction)

XRD and DXRD analysis of the fine sediment fraction from 0.5–1.0 cm depth at all four stations gave essentially the same results. To avoid repetition

of very similar patterns only those for station 5 and 14 are presented. When "reading" the diagrams in Figs. 2–5, it should be kept in mind that (1) peak positions (each mineral is characterized by a "set" of peaks) indicate which mineral has been detected, (2) peak intensities or height may be used to, very roughly, quantify the amount of this mineral, and (3) peak width indicates how well-crystalline a mineral is. As DXRD patterns are obtained by subtraction of the XRD diagram after treatment from the XRD diagram obtained before treatment, minerals that have been dissolved will appear as positive peaks in the pattern.

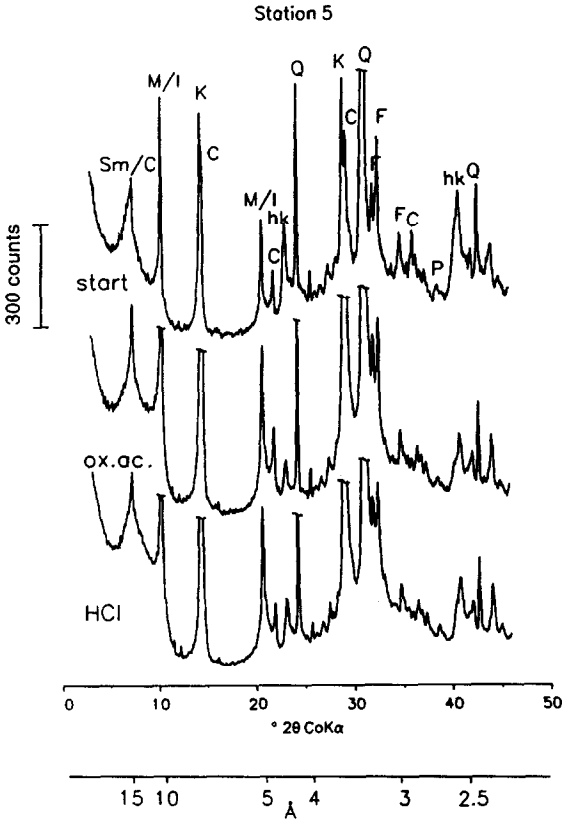

Fig. 2. X-ray powder diffraction (XRD) patterns for the $< 10\ \mu m$ sediment fraction from station 5. Patterns labelled "start", "ox.ac." and "HCl", were made before extraction, after oxalic acid extraction, and after 0.1 M HCl extraction, respectively. Sm = Smectite, C = Chlorite, M/I = Mica/Illite, K = Kaolinite, Q = Quartz, F = Feldspar, P = Pyrite, hk = non-diagnostic clay mineral reflections.

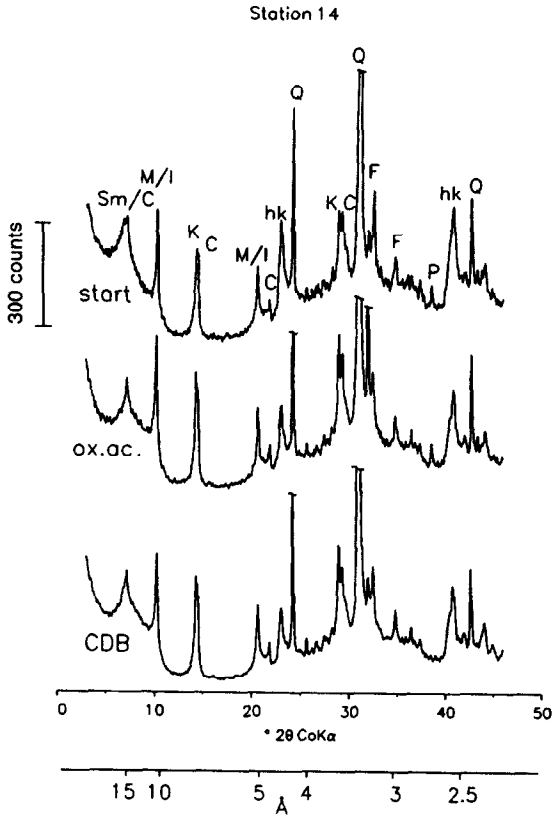

Fig. 3. X-ray powder diffraction (XRD) patterns for the $< 10\ \mu m$ sediment fraction from station 14. Patterns labelled "start", "ox.ac" and "CDB", were made before extraction, after oxalic acid extraction, and after two sequential CDB extractions, respectively. Peak labels as in Fig. 2.

Chlorite, mica/illite, kaolinite, feldspar, pyrite and quartz were identified in all "start" diagrams (Figs. 2 and 3). The broad peak at 15.2 Å, overlain by a small, sharp chlorite peak, is indicative of smectite. The more pronounced broadening of this peak at station 14 (and 13) then at station 5 (and 9) suggests the presence of a poorly crystalline smectite at the first two stations. Based on the peak height a decrease in chlorite, mica/illite and kaolinite contents was observed in the stations sequence: $5 > 9 > 13 \approx 14$. Highest pyrite contents were found at station 13, subsequently decreasing in the stations sequence $14 > 5 \approx 9$.

In the XRD patterns (Figs. 2 and 3), an increase in intensity of the diagnostic clay mineral reflections

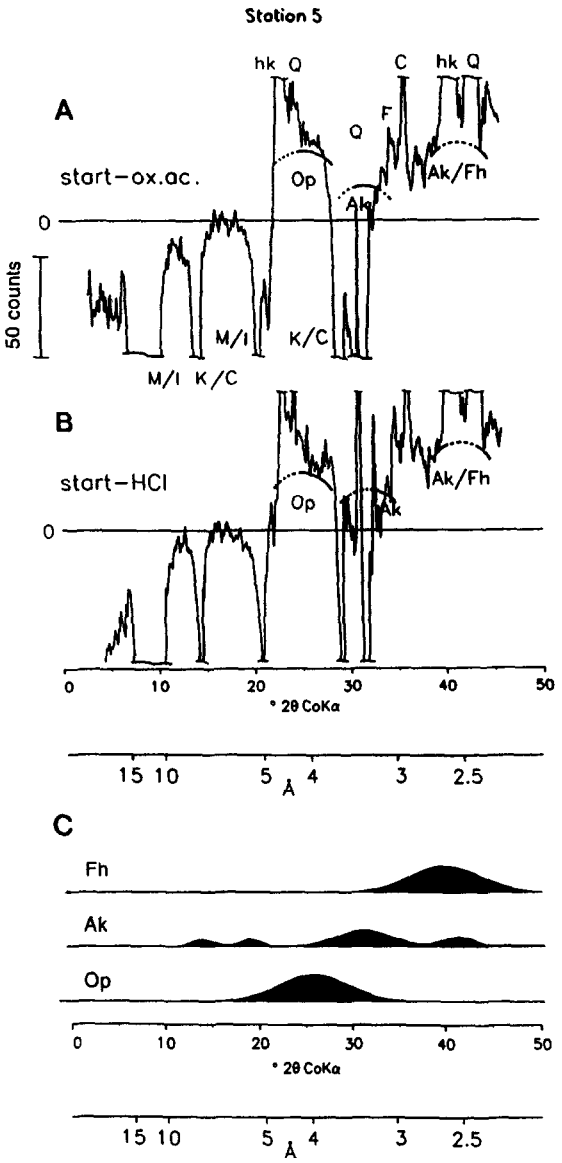

Fig. 4. Differential X-ray powder diffraction (DXRD) patterns for the < 10 μm sediment fraction from station 5. Patterns labelled (A) "start-ox.ac." and (B) "start-HCl", were obtained through subtraction of the "ox.ac." diagram from the "start" diagram and through subtraction of the "HCl" diagram from the "start" diagram. Op = Opal, Fh = Ferrihydrite, Ak = Akageneite. Patterns labelled (C) Op, Fh and Ak are schematic XRD patterns for opal (Van der Gaast, 1991), natural siliceous ferrihydrite (Parfitt et al., 1992) and synthetic akageneite (Schwertmann and Cornell, 1991), respectively. All further peak labels as in Fig. 2.

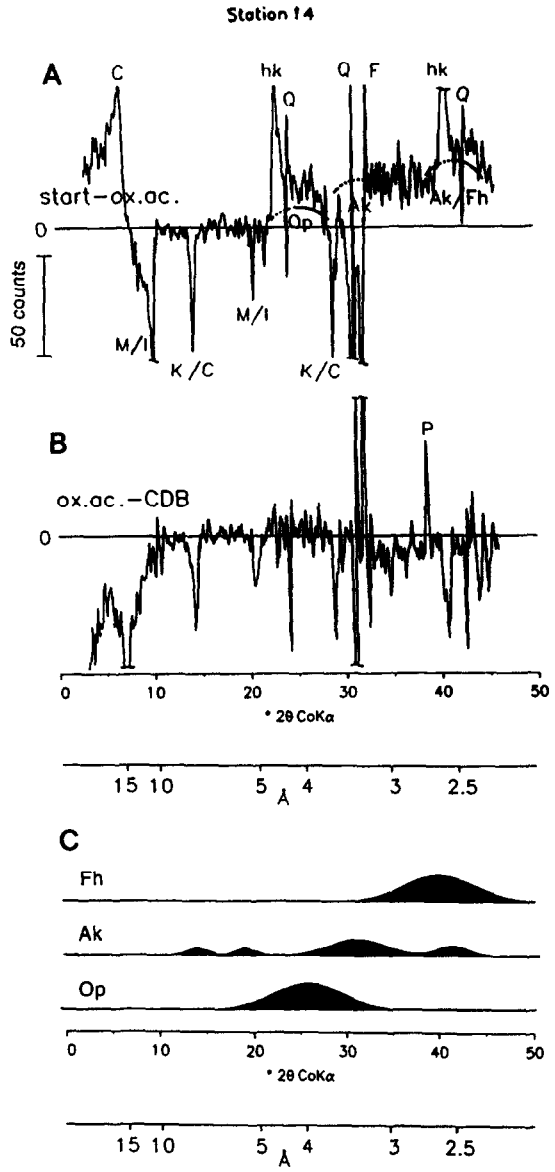

Fig. 5. Differential X-ray powder diffraction (DXRD) patterns for the < 10 μm sediment fraction from station 14. Patterns labelled (A) "start-ox.ac." and (B) "ox.ac-CDB", were obtained through subtraction of the "ox.ac." diagram from the "start" diagram and through subtraction of the "CDB" diagram from the "ox.ac." diagram. Patterns labelled (C) Op, Fh and Ak are schematic XRD patterns for opal (Van der Gaast, 1991), natural siliceous ferrihydrite (Parfitt et al., 1992) and synthetic akageneite (Schwertmann and Cornell, 1991), respectively. All peak labels as in Fig. 2 and 4.

Table 3
Organic C and N contents (in wt.%) in the < 10 μm fraction before and after oxalic acid and 0.1 M HCl extraction

Station	Before extraction		Oxalic acid treated		0.1 M HCl treated	
	Org. C (%)	Org. N (%)	Org. C (%)	Org. N (%)	Org. C (%)	Org. N (%)
5	3.17	0.41	3.63	0.59	4.34	0.46
9	4.05	0.47	4.34	0.46	–	–
13	4.74	0.56	5.35	0.63	–	–
14	4.25	0.54	4.70	0.55	–	–

and a decrease in intensity of the feldspar and quartz and the non-diagnostic (*hk*) clay mineral reflections were observed after oxalic acid and 0.1 M HCl extraction. This resulted in negative peaks at the locations of the diagnostic clay mineral reflections and positive peaks at the locations of the quartz, feldspar and non-diagnostic clay mineral reflections in the corresponding DXRD patterns (Fig. 4A and B and 5A). These peaks are attributed to changes in mineral orientation (see Methods section) and thus do not indicate mineral dissolution. Instead of the expected increase in intensity of the diagnostic chlorite peak at 14.1 Å after the oxalic acid treatment, a decrease was observed at stations 9, 13 and 14

Table 4
Fe, Al, Si, and P (in μmol/g) extracted from the fine sediment fraction (< 10 μm) with 0.1 M HCl (st. 5), NH_4-oxalate and sequentially with oxalic acid and CDB (all stations)

Solution	Station	Fe (μmol/g)	Al (μmol/g)	Si (μmol/g)	P (μmol/g)	Mn (μmol/g)	Fe/Al (mol/mol)	Fe/Si (mol/mol)	Si/Al (mol/mol)	Fe/P (mol/mol)
0.1 M HCl	5	131	167	198	n.d.	1.4	0.8	0.7	1.2	–
NH_4-oxalate	5	166	27	64	19	1.5	6.1	2.6	2.3	8.9
	9	114	27	50	12	1.8	4.2	2.3	1.9	9.4
	13	222	50	80	25	5.5	4.5	2.8	1.6	8.7
	14	211	41	55	19	6.0	5.2	3.8	1.4	11.3
Oxalic acid	5	307	110	52	26	2.5	2.8	5.8	0.5	12
	9	224	98	64	11	1.9	2.3	3.5	0.7	20
	13	287	103	75	23	4.6	2.8	3.8	0.7	12
	14	290	97	89	21	5.3	3.0	3.3	0.9	14
CDB-I	5	145	48	235	5.7	0.8	3.0	0.6	4.9	25
	9	125	55	321	6.1	0.5	2.2	0.4	5.8	21
	13	109	58	539	6.3	0.8	1.9	0.2	9.3	17
	14	107	59	426	6.7	0.6	1.8	0.3	7.2	16
CDB-II	5	29	31	81	0	0	0.9	0.4	2.6	–
	9	27	29	85	0	0	0.9	0.3	2.9	–
	13	26	33	201	0	0	0.8	0.1	6.1	–
	14	26	32	164	0	0	0.8	0.2	5.2	–
Sum	5	482	189	369	31	3.3	2.5	1.3	2.0	15
	9	375	183	470	17	2.4	2.1	0.8	2.6	22
	13	422	194	814	29	5.4	2.2	0.5	4.2	14
	14	423	188	680	28	5.9	2.3	0.6	3.6	15

(shown for station 14 in Fig. 3), resulting in positive peaks in the DXRD patterns (shown for station 14 in Fig. 5A). This suggests dissolution of chlorite or alteration of the chlorite Fe/Mg-hydroxide interlayer upon oxalic acid extraction.

All DXRD patterns obtained after the oxalic acid extraction, as shown for stations 5 and 14 (Fig. 4A and Fig. 5A), showed several broad bulges (indicated with curved lines) underlying the sharper reflection peaks. Similar broad bulges were obtained in the DXRD patterns after the 0.1 M HCl extraction at station 5 (Fig. 4B). These broad bulges suggest dissolution of poorly crystalline material with oxalic acid and 0.1 M HCl. The positions of the bulges in the DXRD patterns in Fig. 4A and B and Fig. 5A, suggest dissolution of opal (4.1 Å), ferrihydrite (2.6 Å) and akageneite (2.5 and 3.3 Å). Schematic XRD patterns for opal (Van der Gaast, 1991), natural siliceous ferrihydrite (Parfitt et al., 1992) and synthetic akageneite (Schwertmann and Cornell, 1991) are shown in Fig. 4C and Fig. 5C for comparison. The 5.3 and 7.4 Å reflections (at 19 and 14°2θ) observed for synthetic akageneite by Schwertmann and Cornell (1991) are weak or absent in our patterns. At the presence, width and intensity of the observed reflections are a direct result of the morphology of the particles, the akageneite in our samples may be of different morphology than the synthetic akageneite of Schwertmann and Cornell (1991).

As removal of several wt.% of organic matter may also give this type of bulges in DXRD patterns (Van der Gaast, 1991), the effect of oxalic acid and 0.1 M HCl on organic material was addressed. Organic C and N contents on average increased ~ 10% upon extraction with oxalic acid (Table 3). After the 0.1 M HCl extraction for station 5 a similar increase in organic N and even a larger increase in organic C (~ 25%) was found. The increase can be explained by weight loss during extraction due to dissolution of Fe oxides (upto ~ 5 wt.%) and other compounds. Obviously, extraction of organic material cannot account for the (positive) bulges in Fig. 4A and B and Fig. 5A. We conclude that, although identification of ferrihydrite and akageneite based on one or two broad peaks remains provisional, it is the most likely explanation for the observed DXRD patterns.

After two extractions with the CDB-solution (only shown for station 14 in Fig. 5B), the intensity of the diagnostic clay mineral reflections (especially chlorite) further increased. All DXRD patterns showed almost complete removal of pyrite, as shown for station 14 in Fig. 5B.

3.2. Chemistry of sediment extractions (< 10 μm fraction)

The sum of the Fe extracted by consecutive oxalic acid and CDB treatments varied between 375 (st. 9) and 482 μmol/g (st. 5) or 2.1–2.7 wt.% Fe (Table 4). Most Fe (60–69% of total extracted Fe) was dissolved in the oxalic acid step. Oxalic acid always extracted more Fe than NH_4-oxalate (a factor 1.8 and 2.0, and 1.3 and 1.4 at stations 5 and 9, and 13 and 14, respectively), whereas NH_4-oxalate extracted only slightly more (1.2 times) Fe than 0.1 M HCl (st. 5).

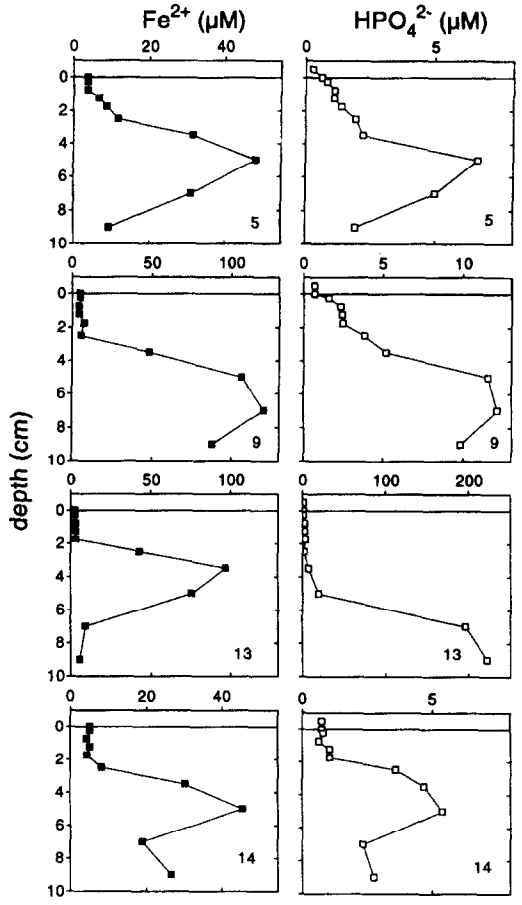

Fig. 6. Pore water profiles of Fe^{2+} and HPO_4^{2-} (μmol l^{-1}) at the four stations.

Of the total extractable Al and Si, oxalic acid extracted 52–58% and 9–14%, respectively. The remaining extractable Al and Si was extracted in the two following CDB steps. No large differences between stations could be observed for oxalic acid and CDB-extractable Al. CDB-extractable Si showed a clear gradient, however, decreasing in the station sequence: 13 > 14 > 9 > 5. Generally, the amount of Fe extracted relative to Al and Si decreased with each successive extraction step resulting in a decrease in Fe/Al and Fe/Si ratios.

Oxalic acid dissolved 64–86% of total extractable P. The remaining P was dissolved in the first CDB step. Generally, very similar amounts were extracted at all stations, both with oxalic acid and NH_4-oxalate. Only at station 9 less P was extracted than at the other stations (11 versus 19–25 μmol/g). Fe/P ratios at all stations were very similar ($\sim$ 9–11 for NH_4-oxalate, $\sim$ 12–14 for oxalic acid with the exception of the value of 20 for station 9). Fe/P ratios for the first CDB step ranged from 16 to 25. 77–90% of total Mn was extracted in the oxalic acid step. Mn contents at stations 5 and 9 are a factor 2 lower than at stations 13 and 14.

Of the non-sequential extraction procedures used, oxalic acid extracted the most Fe at all stations. Much less Fe was extracted in the two following CDB extractions. No clear relationship was observed between extracted Fe and Si, Al and Mn.

3.3. Pore water profiles

Pore water profiles of Fe^{2+} and HPO_4^{2-} (Fig. 6), and solid phase and pore water profiles of Mn^{2+} (not shown) indicate the presence of an oxidized surface layer at all stations. This is confirmed by simultane-

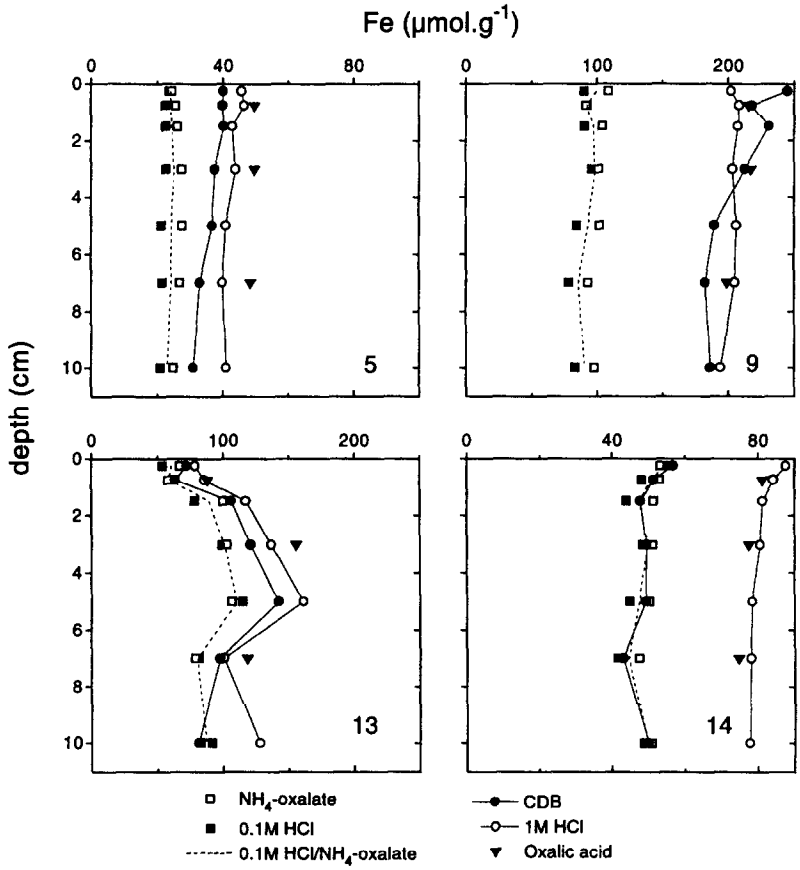

Fig. 7. Solid phase profiles of Fe (μmol g^{-1}) as obtained with five (non-sequential) extraction procedures.

ously measured NO_3^- profiles (Lohse et al., 1995), which show that nitrate was virtually absent below 2–3 cm depth at all stations. Here, pore water Fe^{2+} (Fig. 6) reaches maximum values of ~ 50 μmol l^{-1} at the sandy stations (5 and 14) and ~ 120 and ~ 100 μmol l^{-1} at the silty stations (9 and 13). At all stations Fe^{2+} concentrations drop sharply to relatively constant values between 2.5 and 5 μmol l^{-1} in the oxidized surface layer, implying precipitation of Fe^{2+} in the upper 2–3 cm of the sediment. Pore water HPO_4^{2-} profiles show a strong resemblance to the Fe^{2+} profiles at stations 5, 9 and 14, with maximum values which are a factor 7–10 lower than those for Fe^{2+}, and relatively constant values in the oxidized surface layer between 0.8 and 2 μmol l^{-1}. At station 13, much higher HPO_4^{2-} concentrations (~ 200 μmol l^{-1}) and a decoupling of pore water Fe^{2+} and HPO_4^{2-} is observed.

3.4. Solid phase profiles

Solid phase profiles of Fe obtained with the various extraction solutions are shown for each location in Fig. 7. NH_4-oxalate extracted ~ 10% more Fe than 0.1 M HCl, but both extractants give similar profiles. Oxalic acid extracted 1.8–2.4 and 1.5–1.6 times more Fe than NH_4-oxalate at stations 5 and 9, and 13 and 14, respectively. Oxalic acid extracted equal or higher amounts of Fe compared to 1 M HCl but overall, there was a good correlation (Fe-oxalic acid = 1.08 × Fe-1 M HCl − 1.12; $R^2 = 0.98$, $n = 12$). CDB dissolved similar amounts of Fe as NH_4-oxalate and 0.1 M HCl at station 13 (3 depths) and 14, but much higher amounts at stations 5 and 9. The profile shapes obtained with the 5 methods are quite consistent at stations 13 and 14, but are much more variable at stations 5 and 9. Sediment analysis (par-

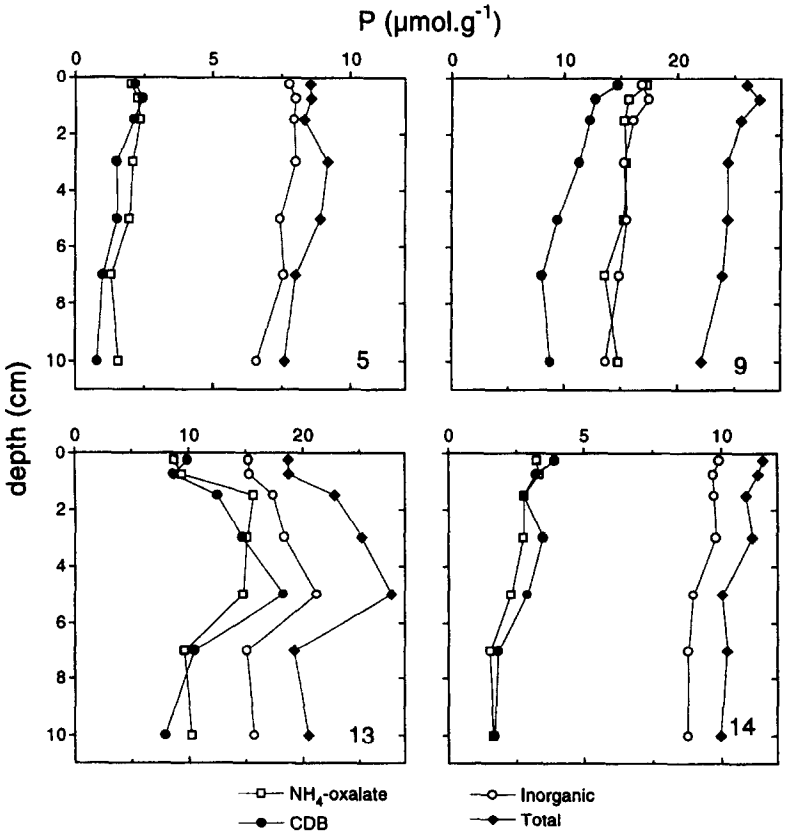

Fig. 8. Solid phase profiles of P (μmol g^{-1}) as obtained with four (non-sequential) extraction procedures.

ticle size, porosity, organic C, N, P, microscopic examination (8–50× magnification)) indicated an enrichment in aggregated particles (presumably faecal pellets) comprised of fine material between 1.5 and 7 cm at station 13. This observed enrichment correlates with the high extractable Fe, suggesting a relationship.

Extraction with CDB (which gives a measure of Fe-bound P) and NH_4-oxalate resulted in similar profiles for P at stations 5, 13 and 14 (Fig. 8). At station 9, however, much more P was extracted with NH_4-oxalate than with CDB and the profile of NH_4-oxalate P was almost identical to that of inorganic P. This indicates that NH_4-oxalate dissolved apatite P besides Fe-bound P at this station. Fe-bound P and inorganic P both show a decrease with depth at stations 5, 9 and 14. Only at station 9 the decrease of Fe-bound P is significantly larger than that of inorganic P (and total P), suggesting an increase of another inorganic phase containing P with depth. From the difference between inorganic and CDB P this non-Fe-bound inorganic P phase can be estimated to increase from ~ 2 μmol g^{-1} in the surface sediment to ~ 7 μmol g^{-1} in deeper layers. Fe-bound P on average accounts for ~ 21 and 30%, and ~ 68 and 70% of inorganic P at the sandy (5 and 14) and silty (13 and 9) stations, respectively. Total P profiles relative to those for inorganic P suggest a slight decrease of organic P with depth at stations 9 and 14 and an enrichment of organic P between 1.5 and 7 cm at stations 5 and 13. Organic P on average contributes to 10 and 12%, and 22 and 37% of total P at the sandy (5 and 14) and silty (13 and 9) locations, respectively.

4. Discussion

4.1. Sediment composition (< 10 μm fraction)

The similar mineralogical composition of the fine sediment fraction at all four locations suggests a common source for most of the deposited fine material. This is in line with the large contribution (up to 85%) of well-mixed North Atlantic, Channel and seafloor erosion derived material to suspended matter transported through the North Sea (Eisma and Kalf, 1987). The suggested presence of a poorly crystalline smectite at the German Bight stations (13, 14) may be indicative of the contribution of more local sources in this area (Irion et al., 1987).

The much higher Mn (Table 4) and pyrite contents (Figs. 2 and 3) in the fine sediment at stations 13 and 14 (German Bight) can be attributed to diagenetic processes as these sediments become completely anoxic in summer in contrast to stations 5 and 9 (Oystergrounds and Skagerrak, respectively) (Lohse et al., 1995). Despite their difference in grain-size, a greater degree of consistency between the Fe extraction results (e.g. NH_4-oxalate and oxalic acid Fe ratios) was observed for stations 13 and 14 than for stations with a more comparable grain size (st. 9 and 5, respectively). This could also be explained by diagenetic processes. A higher clay mineral content of the fine sediment fraction at the latter stations, and perhaps a different clay mineral composition are more likely explanations, however, as will become clear from the calibration of the Fe extractions with DXRD further in the text.

4.2. Identification of Fe oxides with DXRD (< 10 μm fraction)

The results of the DXRD analysis (Figs. 4 and 5) indicate that both poorly crystalline ferrihydrite and akageneite were dissolved with oxalic acid and 0.1 M HCl during the extraction of the fine sediment fraction. Results from laboratory and field studies suggest that both ferrihydrite and akageneite could form under conditions typical for coastal marine environments. Ferrihydrite is a relatively common Fe oxide in soil and sediment environments where oxidizing and reducing conditions alternate and hence an active Fe turnover exists (Schwertmann, 1988a; Schwertmann and Cornell, 1991). Inhibitors, such as phosphate, silicate and organics are known to stabilize ferrihydrite and to retard its transformation into more crystalline minerals (Karim, 1984; Cornell, 1985; Cornell et al., 1987; Schwertmann and Cornell, 1991). Akageneite, in contrast, is very rare in soils. The conditions for formation of akageneite in the marine environment are favourable, however, as high Cl^- (or F^-) concentrations are a prerequisite for its formation (Childs et al., 1980; Schwertmann and Cornell, 1991). Murray (1978) found it to be the form of Fe that precipitates from Fe^{3+} in seawater

and suggested (Murray, 1979) that hydrolysis of Fe^{2+} in seawater may also produce akageneite.

No evidence for the presence of goethite, which is the most probable crystalline Fe oxide in temperate regions (Schwertmann, 1988a), was found in the XRD or DXRD patterns. As the detection limit for goethite in our laboratory is ~ 0.5% wt.% (55 μmol g^{-1}), it can account for some but not all of the Fe dissolved during the two CDB extractions. At stations 13 and 14 pyrite dissolution (~ 1 wt.% FeS_2 = 83 μmol g^{-1}) contributes substantially to extracted Fe, as indicated by the DXRD diagram for station 14 (Fig. 5), which showed almost complete removal with CDB. Due to the low pyrite contents at stations 5 and 9, another source should be responsible for most of the extracted Fe there. The dissolution of pyrite by CDB was unexpected (Table 2; Kostka and Luther, 1994), but may be explained by the strong complexing activity of the citrate and, possibly, by instability of the pyrite in the oxidized environment of the surface sediment. Again, this illustrates the pitfalls involved in the use of extraction procedures for natural sediments.

4.3. Calibration of the extraction procedures for bulk sediment samples

Oxalic acid dissolved Al, Si, Fe and P in similar proportions both from the fine sediment fraction and from the bulk sediment samples (Fig. 9A). This was also the case for NH_4-oxalate extractable Al, Fe and P (Fig. 9B). Only NH_4-oxalate extractable Si contents relative to Fe (and Al) were grain size dependent. Ratios of NH_4-oxalate and oxalic acid extractable Fe were similar for the fine (1.8 and 2.0, and 1.3 and 1.4 at stations 5 and 9, and 13 and 14, respectively) and bulk sediment (1.8 and 2.4, and 1.5 and 1.6). This implies that the same Fe phases were dissolved from the fine and bulk sediment samples with both extractants. Thus it is possible to use the DXRD and extraction results for the < 10 μm fraction as a calibration of the non-sequential extraction procedures for Fe for bulk sediment samples.

Only a fraction of total sediment Al and Si was extracted with oxalic acid, NH_4-oxalate and CDB. Due to the large differences in affinity of oxalate and citrate for Al, Si and Fe (Furrer and Stumm, 1986; Bennett, 1991; Kodama and Ross, 1991) and the many mineral sources possible (besides Fe oxides also clay minerals, amorphous silica, quartz), the quantity of Al and Si extracted and the Fe/Al, Fe/Si and Si/Al ratios cannot be used for direct identification of Fe sources in the extractions. For example, it is apparent that CDB-I–Fe and CDB-I–Si have a different source (Table 4), given the fact that samples from stations where the highest quantities of Fe were dissolved showed the least release of Si, and vice versa. All calibration is thus solely based on the amount of Fe extracted with each procedure and the DXRD results.

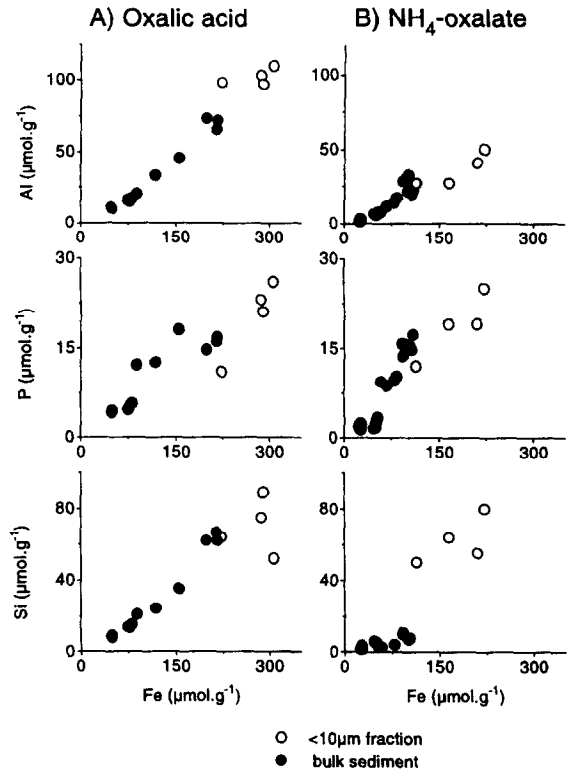

Fig. 9. Relationship between the quantity of Fe, Al, P, and Si extracted from the fine sediment fraction (open circles) and from bulk sediment samples (filled circles) at all four stations using (A) oxalic acid and (B) NH_4-oxalate.

The DXRD diagrams for the < 10 μm fraction from station 5 indicate that ferrihydrite and akageneite were dissolved both with 0.1 M HCl and oxalic acid (Figs. 4 and 5). The amount of Fe extracted with 0.1 M HCl was less than half of that extracted with oxalic acid (Table 4). A good correlation between 0.1 M HCl Fe and NH_4-oxalate Fe was

observed (Fig. 7). This suggests that (1) 0.1 M HCl Fe and NH_4-oxalate Fe are both a good measure for the ferrihydrite and akageneite content in these sediments, and that (2) oxalic acid extracts additional Fe from another source. The ratios of NH_4-oxalate/oxalic acid Fe indicate that this source is more important at stations 5 and 9 than at stations 13 and 14.

The CDB extractions cannot be calibrated in a similar manner, as the extraction of the < 10 μm fraction was performed as part of a sequential extraction scheme, in contrast to the non-sequential bulk sediment extractions. It is clear, however, that the various sources of Fe in the < 10 μm fraction and in the bulk sediment samples do not contribute to CDB Fe in similar proportions. Pyrite dissolution accounts for an important part of CDB Fe in the < 10 μm fraction at stations 13 and 14. CDB, 0.1 M HCl and NH_4-oxalate Fe were approximately equal in the bulk sediment samples at these stations (Fig. 7). Therefore, pyrite dissolution cannot contribute substantially to the CDB Fe extracted from the bulk sediment samples either at stations 13 and 14 or 5 and 9. This is in line with previous observations that bulk sediment pyrite contents in North Sea sediments are low (Jørgensen, 1989; Canfield et al., 1993). As CDB Fe was substantially higher than 0.1 M HCl and NH_4-oxalate Fe in the bulk sediment extractions for stations 5 and 9 (Fig. 7), this leaves us with an unknown source of CDB Fe at these locations.

As mentioned earlier, goethite may account for some but not all of this CDB Fe. Minor quantities of Fe^{2+} are known to catalyze the reduction and dissolution of crystalline Fe oxides in the presence of oxalate (Sulzberger et al., 1989; Kostka and Luther, 1994). This catalysis reaction does not occur when using 0.1 M HCl as an extractant for poorly crystalline Fe oxides. The good correlation between 0.1 M HCl and NH_4-oxalate Fe at all stations and the much higher quantities of CDB Fe at stations 5 and 9 suggest that this catalysis reaction did not occur during the oxalate extraction. This provides further support for only a minor contribution of crystalline Fe oxides to CDB Fe.

Both oxalic acid and CDB may extract Fe from chlorite interlayers (Harward and Theisen, 1962; Weaver and Pollard, 1972). The higher chlorite content of the sediments at stations 5 and 9 relative to those of stations 13 and 14 supports the role of chlorite as an important source of the "extra" Fe. Additional evidence in the case of the oxalic acid extraction is provided by the alteration of the chlorite peaks in the DXRD patterns (Fig. 5A), and the good correlation of oxalic-acid extractable Fe with 1 M HCl extractable-Fe (bulk sediment extractions; Fig. 7), as 1 M HCl should dissolve some fraction of the clay minerals but not the most crystalline Fe oxides (Table 2).

Combining these results with the Fe profiles in Fig. 7, we conclude that at stations 13 and 14, ferrihydrite and akageneite are practically the only Fe oxide phases present. At stations 5 and 9, ferrihydrite and akageneite are also present but account for only ~ 65 and $\sim 50\%$ of CDB-Fe in the surface sediment. Remarkably, NH_4-oxalate and 0.1 M HCl extractable Fe show no gradient with depth at stations 5 and 9, whereas CDB-Fe does. Substantial release of Fe from clay minerals upon burial at these locations is unlikely (e.g. Hathaway, 1979). Incomplete extraction of the less crystalline Fe oxides by the NH_4-oxalate and 0.1 M HCl, e.g., due to protection by adsorbed Si, P or organics (Karim, 1984; Borggaard, 1991; Schwertmann, 1991), is a more probable explanation.

4.4. Fe oxides and the binding of P in North Sea sediments

A close relationship between P adsorption or the amount of Fe-bound P, and the concentration of total or poorly crystalline Fe oxides has been demonstrated frequently for different types of soils and sediments (e.g. Borggaard, 1983b; Jensen and Thamdrup, 1993). Both experiments with natural and synthetic mineral phases (Borggaard, 1983a and b; Schwertmann, 1988b; Parfitt, 1989; Torrent et al., 1992) have shown that the specific surface area of Fe oxides largely determines their P sorption capacity and intensity and that, due to their larger surface areas, poorly crystalline or "amorphous" Fe oxides have a larger potential for P sorption than more crystalline Fe phases.

Evidence for the dominant role of poorly crystalline Fe oxides in the binding of P in North Sea sediments was obtained by plotting Fe-bound P and the buffer intensity for HPO_4^{2-} (linear adsorption coefficient K at $[HPO_4^{2-}] = 1$ μmol/l, including

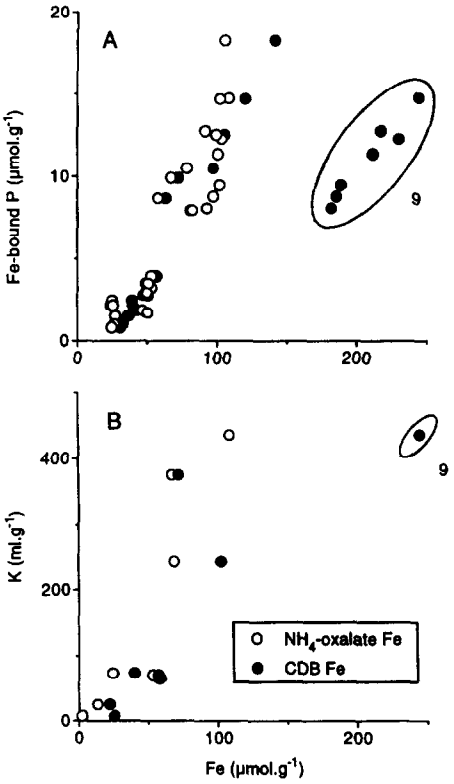

Fig. 10. (A) Relationship between Fe-bound P and NH_4-oxalate (open circles) and CDB (filled circles) extractable Fe at four North Sea stations (Fe-bnd P = 0.15 × NH_4-ox.-Fe − 3.19, R^2 = 0.84, n = 28; Fe-bnd P = 0.16 × CDB-Fe − 4.41, R^2 = 0.96, n = 21, excluding st. 9); (B) Relationship between the linear adsorption coefficient (K) for HPO_4^{2-} and NH_4-oxalate (open circles) and CDB (filled circles) extractable Fe at 8 North Sea stations (K values from Slomp and Van Raaphorst, 1993; K = 4.1 × NH_4-ox.-Fe − 43.6, R^2 = 0.74, K = 3.6 × CDB-Fe − 72.5, R^2 = 0.56, excluding st. 9).

results from four additional stations; Slomp and Van Raaphorst, 1993) versus NH_4-oxalate Fe and CDB Fe (Fig. 10A and B, respectively). K and the concentration of Fe-bound P are well correlated with NH_4-oxalate Fe and CDB Fe at all stations where similar amounts of Fe were extracted with both solutions. At station 9 the "extra" Fe phase (relative to NH_4-oxalate Fe) extracted with CDB apparently had no affinity for P and did not contribute to Fe-bound P. Fe contents at station 5 were too low to enable similar observations. This strongly supports binding of P to poorly crystalline ferrihydrite and akageneite in these sediments, and provides further support for the suggested minor contribution of crystalline Fe oxides to the "extra" CDB Fe at stations 5 and 9, as a contribution to P binding would be expected for crystalline Fe oxides but not necessarily for clay minerals (Krom and Berner, 1980; Parfitt, 1989).

A tight coupling of pore water HPO_4^{2-} and Fe^{2+} was observed at stations 5, 9 and 14. Here, Fe^{2+}/HPO_4^{2-} ratios at maximum pore water concentrations of Fe (~ 7–14) were in the same range as NH_4-oxalate Fe/Fe-bound P ratios for the fine fraction (~ 9–11), and for bulk sediment samples (~ 7–13) from the upper layer, and as Fe/P values known for synthetic poorly crystalline Fe oxides (~ 10; Borggaard, 1983a; Gerke and Hermann, 1992). This suggests that at these three stations pore water HPO_4^{2-} production at the time of core collection (February 1992) was dominated by release from poorly crystalline Fe oxides. Only at station 13, a decoupling of pore water Fe^{2+} and HPO_4^{2-} was observed. At the maximum in pore water Fe^{2+}, the Fe^{2+}/HPO_4^{2-} ratio (~ 13) was still in the range suggesting release from Fe oxides, but at depth in the sediment much higher HPO_4^{2-} concentrations (~ 200 µmol l^{-1}), and much lower Fe^{2+}/HPO_4^{2-} ratios were observed. This suggests a larger production of HPO_4^{2-} due to organic matter mineralization in deeper layers than at the other stations. The NH_4-oxalate Fe/Fe-bound P ratios are comparable to amorphous Fe/Fe-bound P ratios found previously for the Kattegat (~ 8) and Aarhus Bay (~ 8–9) (Jensen and Thamdrup, 1993) and to total Fe-oxide Fe/Fe-bound P (~ 10) in Laurentian Trough sediments (Sundby et al., 1992). Jensen and Thamdrup (1993) found higher amorphous Fe/Fe-bound P ratios (~ 17) in Skagerrak sediment and concluded that here the Fe oxides might be less capable of adsorbing P or were less saturated with P. They determined amorphous Fe as the difference between total Fe extracted with 0.5 M HCl and Fe(II) extracted with oxalate buffer under anoxic conditions. As 0.5 M HCl probably extracts more Fe from clay minerals than NH_4-oxalate (Table 2), and as we found the same high Fe/P ratio of 17 in Skagerrak surface sediment when using CDB or oxalic acid Fe as a measure for Fe in Fe oxides, they probably attributed Fe from clay minerals to amorphous Fe. We conclude that ratios of poorly crystalline Fe oxides and Fe-bound P are very similar (~ 10) in many marine sediments.

HPO_4^{2-} released to the pore water can (1) (re)adsorb to Fe oxides in the upper part of the sediment; (2) escape to the overlying water or (3) precipitate as an authigenic phase in the sediment. The decrease with depth of both Fe-bound and inorganic P at the stations where no net sedimentation of material occurs (st. 5 and 14; Fig. 8) suggests that here most of the P released upon reduction of Fe oxides (Fig. 6) is readsorbed in the upper part of the sediment or released to the overlying water. Only in the depositional area of the Skagerrak (st. 9) a substantial increase of another inorganic phase containing P with depth can be inferred from Fig. 8. Although non-steady state changes in composition of the deposited material cannot be ruled out, this may be indicative of an early diagenetic "sink switching" from Fe oxides to another inorganic phase (e.g. CFA), as has recently been suggested for Laurentian Trough sediments (Lucotte et al., 1994).

Poorly crystalline Fe oxides and Fe-bound P clearly persisted into the reduced zone (down to 10–12 cm), thus making these Fe oxides at least a temporary sink for P in North Sea sediments. Persistence of Fe-bound P with depth (down to 160 cm) at a deeper Skagerrak station (Jensen and Thamdrup, 1993) suggests that poorly crystalline Fe oxides may also form a permanent sink for P, as has been observed for other continental margin sediments (e.g. Berner et al., 1993; Ruttenberg and Berner, 1993). This implies that these Fe oxide forms are protected against reduction, presumably due to coatings with reduced iron compounds (Postma, 1993) and due to the presence of surface bound P, Si and organics (Borggaard, 1991; Biber et al., 1994).

The absence or only minor role of crystalline Fe oxides, such as goethite, in North Sea surface sediments, despite their higher resistance against reduction compared to poorly crystalline phases, can be attributed to three factors. First, there is a relatively low input of terrestrial material adding crystalline Fe oxides in this shelf sea due to trapping of material in estuaries (Eisma et al., 1982; Eisma and Kalf, 1987). Second, long residence times of material on the shelf due to frequent deposition and resuspension prior to burial in the main deposition areas (Eisma and Kalf, 1987), combined with a frequent cycling of Fe between oxidized and reduced Fe forms (Canfield et al., 1993), promote formation of poorly crystalline Fe oxides. Third, inhibition of formation of crystalline Fe oxides in continental margin sediments is expected due to the abundant presence of P, Si and organics (Cornell, 1985; Cornell et al., 1987).

5. Conclusions

In this study, a combination of extraction procedures and X-ray powder diffraction has been used to identify the Fe oxides responsible for the binding of P in four sediments from contrasting environments on a continental margin. Poorly crystalline akageneite and ferrihydrite (extractable with 0.2 M NH_4-oxalate or 0.1 M HCl) were found to be the most important Fe oxides at all locations. A good relationship of both the concentration of Fe-bound P and the linear adsorption coefficient for HPO_4^{2-} with NH_4-oxalate Fe provides evidence for the dominant role of this poorly crystalline ferrihydrite and akageneite in the binding of P in these sediments. The ratios of NH_4-oxalate Fe/Fe-bound P were comparable to values found for synthetic poorly crystalline Fe oxides, and for amorphous Fe or total Fe-oxide/Fe-bound P ratios in other marine sediments. This suggests that ratios of poorly crystalline Fe oxides and Fe-bound P may be very similar (~ 10) in many marine sediments.

Pore water HPO_4^{2-} can be produced both due to organic matter decomposition and due to release from Fe oxides. The tight coupling of pore water Fe^{2+} and HPO_4^{2-} and the observed Fe^{2+}/HPO_4^{2-} ratios at maximum pore water Fe^{2+} concentrations at three locations suggest that here, pore water HPO_4^{2-} production at the time of core collection was dominated by release from poorly crystalline Fe oxides. At the German Bight station, the much higher HPO_4^{2-} levels and decoupling of pore water Fe^{2+} and HPO_4^{2-} suggest a larger direct contribution from mineralization of organic matter to pore water HPO_4^{2-} than at the other sites.

The solid phase P profiles at the stations with no net sedimentation suggest that here HPO_4^{2-} released to the pore water is either readsorbed to Fe oxides in the upper part of the sediment or released to the overlying water. In the Skagerrak, however, the decrease with depth of Fe-bound P and the suggested increase of another inorganic phase containing P,

may indicate an early diagenetic "sink switching" of P.

The persistence of poorly crystalline Fe oxides and Fe-bound P with depth, as observed in this study, is in line with the large range in susceptibility to reduction known for Fe oxides in sediments. This enables these Fe phases to act as both a temporary and permanent sink for P in continental margin sediments.

Acknowledgements

We thank the crew of R.V. *Pelagia* for their help during the cruise and A.J.J. Sandee, H.T. Klooster-huis and J.F.P. Malschaert for the grain size analysis, (in)organic C and N analysis and collection of pore water. We closely cooperated with L. Lohse, who studied N cycling in the same sediments. The cruise (BELS 92) was financially supported by the Netherlands Marine Research Foundation (NWO-SOZ grant 39104). The manuscript benefited from the reviews of K.C. Ruttenberg and M.E. Lebo.

References

Anton, K.K., Liebezeit, G., Rudolph, C. and Wirth, H., 1993. Origin, distribution and accumulation of organic carbon in the Skagerrak. Mar. Geol., 111: 287–297.

Aspila, K.I., Agemian, H. and Chau, A.S.Y., 1976. A semi-automated method for the determination of inorganic, organic and total phosphate in sediments. Analyst, 101: 187–197.

Bennett, P.C., 1991. Quartz dissolution in organic-rich aqueous systems. Geochim. Cosmochim. Acta, 55: 1781–1797.

Berner, R.A., Ruttenberg, K.C., Ingall, E.D. and Rao, J.-L., 1993. The nature of phosphorus burial in modern marine sediments. In: R. Wollast et al. (Editors), Interactions of C, N, P and S Biogeochemical Cycles and Global Change. NATO ASI Ser., 14. Springer, Berlin, pp. 365–378.

Biber, M.V., Dos Santos Afonso, M. and W. Stumm, 1994. The coordination chemistry of weathering: IV. Inhibition of the dissolution of oxide minerals. Geochim. Cosmochim. Acta, 58: 1999–2010.

Borggaard, O.K., 1983a. Effect of surface area and mineralogy of iron oxides on their surface charge and anion-adsorption properties. Clays Clay Miner., 31: 230–232.

Borggaard, O.K., 1983b. The influence of iron oxides on phosphate adsorption by soil. J. Soil Sci., 34: 333–341.

Borggaard, O.K., 1991. Effects of phosphate on iron oxide dissolution in ethylenediamine-N,N,N′,N′-tetraacetic acid and oxalate. Clays Clay Miner., 39: 324–328.

Burns, R.G. and Burns, V.M., 1980. Manganese oxides. In: R.G. Burns (Editor), Marine Minerals. Reviews in Mineralogy, 6. Mineral. Soc. Am., pp. 1–46.

Canfield, D.E., 1988. Sulfate reduction and the diagenesis of iron in anoxic sediments. Ph.D. dissertation, Yale Univ., New Haven, CT.

Canfield, D.E., 1989. Reactive iron in marine sediments. Geochim. Cosmochim. Acta, 53: 619–632.

Canfield, D.E., Thamdrup, B. and Hansen, J.W., 1993. The anaerobic degradation of organic matter in Danish coastal sediments: iron reduction, manganese reduction and sulfate reduction. Geochim. Cosmochim. Acta, 57: 3867–3883.

Chao, T.T. and Zhuo, L., 1983. Extraction techniques for selective dissolution of amorphous iron oxides from soils and sediments. Soil Sci. Soc. Am. J., 47: 225–232.

Childs, C.W., Goodman, B.A., Paterson, E. and Woodhams, F.W.D., 1980. The nature of iron in akageneite (β-FeOOH). Aust. J. Chem., 33: 15–26.

Cornell, R.M., 1985. Effect of simple sugars on the alkaline transformation of ferrihydrite into goethite and hematite. Clays Clay Miner., 33: 219–227.

Cornell, R.M., Giovanoli, R. and Schindler, P.W., 1987. Effect of silicate species on the transformation of ferrihydrite into goethite and hematite in alkaline media. Clays Clay Miner., 35: 21–28.

Cornwell, J.C. and Morse, J.W., 1987. The characterization of iron sulfide minerals in anoxic marine sediments. Mar. Chem., 22: 193–206.

Duinker, J.C., Van Eck, G.T.M. and Nolting, R.F., 1974. On the behaviour of copper, zinc, iron and manganese and evidence for mobilization processes in the Dutch Wadden Sea. Neth. J. Sea Res., 8: 214–239.

Eisma, D., Cadee, G.C. and Laane, R., 1982. Supply of suspended matter and particulate and dissolved organic carbon from the Rhine to the coastal North Sea. Mitt. Geol.-Paläontol. Inst. Univ. Hamburg, 52: 483–505.

Eisma, D. and Kalf, J., 1987. Dispersal, concentration and deposition of suspended matter in the North Sea. J. Geol. Soc. London, 144: 161–178.

Furrer, G. and Stumm, W., 1986. The coordination chemistry of weathering: I. Dissolution kinetics of δ-Al_2O_3 and BeO. Geochim. Cosmochim. Acta, 50: 1847–1860.

Gerke, J. and Hermann, R., 1992. Adsorption of orthophosphate to humic–Fe-complexes and to amorphous Fe-oxide. Z. Pflanzenernähr. Bodenk., 155: 233–236.

Harward, M.E. and Theisen, A.A., 1962. Problems in clay mineral identification by X-ray diffraction. Soil Sci. Soc. Proc., 26: 335–341.

Hathaway, J.C., 1979. Clay minerals. In: R.G. Burns (Editor), Marine Minerals. Reviews in Mineralogy, 6. Mineral. Soc. Am., pp. 123–150.

Irion, G., Wunderlich, F. and Schwedhelm, E., 1987. Transport of clay minerals and anthropogenic compounds into the German Bight and the provenance of fine- grained sediments SE of Helgoland. J. Geol. Soc. London, 144: 153–160.

Jensen, H.S. and Thamdrup, B., 1993. Iron-bound phosphorus in marine sediments as measured by bicarbonate–dithionite extraction. Hydrobiologia, 253: 47–59.

Jørgensen, B.B., 1989. Sulfate reduction in marine sediments from the Baltic Sea–North Sea transition. Ophelia, 31: 1–15.

Karim, Z., 1984. Characteristics of ferrihydrites formed by oxidation of $FeCl_2$ solutions containing different amounts of silica. Clays Clay Miner., 32: 181–184.

Kauffman, K. and Hazel, F., 1975. Infrared and Mössbauer spectroscopy, electron microscopy and chemical reactivity of ferric chloride hydrolysis products. J. Inorg. Nucl. Chem., 37: 1139–1148.

Kodama, H. and Ross, G.J., 1991. Tiron dissolution method used to remove and characterize inorganic components in soils. Soil. Soc. Am. J., 55: 1180–1187.

Kostka, J.E. and Luther, III, G.W., 1994. Partitioning and speciation of solid phase iron in saltmarsh sediments. Geochim. Cosmochim. Acta, 58: 1701–1710.

Krom, M.D. and Berner, R.A., 1980. Adsorption of phosphate in anoxic marine sediments. Limnol. Oceanogr., 25: 797–806.

Lohse, L., Malschaert, J.F.P., Slomp, C.P., Helder, W. and Van Raaphorst, W., 1995. Sediment–water fluxes of inorganic nitrogen compounds along the transport route of organic matter in the North Sea. Ophelia, 41: 173–197.

Lord, C.J., 1982. A selective and precise method for pyrite determination in sedimentary materials. J. Sediment. Petrol., 52: 664–666.

Lucotte, M. and d'Anglejan, B., 1985. A comparison of several methods for the determination of iron hydroxides and associated orthophosphates in estuarine particulate matter. Chem. Geol., 48: 257–264.

Lucotte, M., Mucci, A. and Hillairemarcel, A., 1994. Early diagenetic processes in deep Labrador Sea sediments — reactive and nonreactive iron and phosphorus. Can. J. Earth Sci., 31: 14–27.

McKeague, J.A. and Day, J.H., 1966. Dithionite- and oxalate-extractable Fe and Al as aids in differentiating various classes of soils. Can. J. Soil Sci., 46: 13–22.

Mehra, O.P. and Jackson, M.L., 1960. Iron oxide removal from soils and clays by a dithionite–citrate system buffered with sodium bicarbonate. Clays Clay Miner., 7: 317–327.

Moore, D.M. and Reynolds, R.C., 1989. X-ray diffraction and the identification and analysis of clay minerals. Oxford Univ. Press, Oxford.

Murray, J.W., 1978. β-FeOOH in marine sediments. Eos, 59: 411–412.

Murray, J.W., 1979. Iron oxides. In: R.G. Burns (Editor), Marine Minerals. Reviews in Mineralogy, Vol. 6. Mineral. Soc. Am., pp. 47–98.

Parfitt, R.L., 1989. Phosphate reactions with natural allophane, ferrihydrite and goethite. J. Soil Sci., 40: 359–369.

Parfitt, R.L., Van der Gaast, S.J. and Childs, C.W., 1992. A structural model for natural siliceous ferrihydrite. Clays Clay Miner., 40: 675–681.

Pettijohn, F.J. and Potter, P.E., 1972. Sand and Sandstone. Springer, New York, NY.

Postma, D., 1993. The reactivity of iron oxides in sediments: a kinetic approach. Geochim. Cosmochim. Acta, 57: 5027–5034.

Ruttenberg, K.C., 1992. Development of a sequential extraction method for different forms of phosphorus in marine sediments. Limnol. Oceanogr., 37: 1460–1482.

Ruttenberg, K.C., 1993. Reassessment of the oceanic residence time of phosphorus. Chem. Geol., 107: 405–409.

Ruttenberg, K.C. and Berner, R.A., 1993. Authigenic apatite formation and burial in sediments from non-upwelling, continental margin environments. Geochim. Cosmochim. Acta, 57: 991–1007.

Saager, P.M., Sweerts, J.P. and Ellermeijer, H.J., 1990. A simple pore-water sampler for coarse sandy sediments of low porosity. Limnol. Oceanogr., 35: 747–751.

Schulze, D.G., 1981. Identification of soil iron minerals by differential X-ray diffraction. Soil Sci. Soc. Am. J., 45: 437–440.

Schwertmann, U., 1988a. Occurrence and formation of iron oxides in various pedoenvironments. In: J.W. Stucki et al. (Editors), Iron in Soils and Clay Minerals. Reidel, Dordrecht, pp. 267–308.

Schwertmann, U., 1988b. Some properties of soil and synthetic oxides. In: J.W. Stucki et al. (Editors), Iron in Soils and Clay Minerals. Reidel, Dordrecht, pp. 203–250.

Schwertmann, U., 1991. Solubility and dissolution of iron oxides. Plant Soil, 130: 1–25.

Schwertmann, U. and Cornell, R.M., 1991. Iron Oxides in the Laboratory. VCH.

Slomp, C.P. and Van Raaphorst, W., 1993. Phosphate adsorption in oxidized marine sediments. Chem. Geol., 107: 477–480.

Strickland, J.D. and Parsons, T.R., 1972. A Practical Handbook of Seawater Analysis, 2nd ed. Bull. Fish. Res. Bd. Can., 167: 1–311.

Sulzberger, B., Suter, D., Siffert, C., Banwart, S. and Stumm, W., 1989. Dissolution of Fe(III)(hydr)oxides in natural waters; Laboratory assessment on the kinetics controlled by surface coordination. Mar. Chem., 28: 127–144.

Sundby, B., Gobeil, C., Silverberg, N. and Mucci, A., 1992. The phosphorus cycle in coastal marine sediments. Limnol. Oceanogr., 37: 1129–1145.

Torrent, J., Schwertmann, U. and Barrón, V., 1992. Fast and slow phosphate sorption by goethite-rich natural materials. Clays Clay Miner., 40: 14–21.

Van der Gaast, S.J., 1991. Mineralogical analysis of marine particles by X-ray powder diffraction. Geophys. Monogr., 63: 343–362.

Van Raaphorst, W. and Kloosterhuis, H.T., 1994. Phosphorus sorption in surficial intertidal sediments. Mar. Chem., 48: 1–16.

Van Weering, T.C.E., Berger, G.W. and Kalf, J., 1987. Recent sediment accumulation in the Skagerrak, northeastern North Sea. Neth. J. Sea Res., 21: 77–189.

Verardo, D.J., Froelich, P.N. and McIntyre, A., 1990. Determination of organic carbon and nitrogen in sediments using the Carlo Erba Na-1500 analyzer. Deep-Sea Res., 37: 157–165.

Von Haugwitz, W., Wong, H.K. and Salge, U., 1988. The mud area southeast of Helgoland: A seismic study. Mitt. Geol.-Paläontol. Inst. Univ. Hamburg., 65: 409–422.

Wang, H.D., White, G.N., Turner, F.T. and Dixon, J.B., 1993. Ferrihydrite, lepidocrocite and goethite in coatings from East Texas vertic soils. Soil Sci. Soc. Am. J., 57: 1381–1386.

Weaver, C.E. and Pollard, L.D., 1972. The Chemistry of Clay Minerals. Elsevier, Amsterdam.